TIME SERIES OF MICROPHYSICAL STRUCTURE AND LIGHTNING POLARITY OF A GROUP OF 334 THUNDERCLOUDS GENERATED SUCCESSIVELY IN A LINE-SHAPED AREA

Takeharu Kouketsu, Hiroshi Uyeda and Tadayasu Ohigashi
HydrosphericAtmospheric Research Center, Nagoya University, Nagoya, Japan

1. INTRODUCTION

It is important to examine the structure of thunderclouds to understand the mechanisms of severe weather such as lightning, heavy rain, hail, tornadoes. Polarimetric weather radars are useful instruments for obtaining microphysical information about precipitation and they have been used for hydrometeor classification (hereafter, HC).

We have developed a HC method for X-band polarimetric radars (X-pols) and have tried HC (Kouketsu and Uyeda, 2010). To validate our HC method, we used simultaneous data from an X-pol and in situ observations of balloon-borne instruments (Kouketsu et al., 2013).

With our HC method, we have examined the microphysical structure of a simple thundercloud (Kouketsu et al., 2011). The volume of the region where the dominant hydrometeor type was expected to be graupel (or ice crystal) around or above -10°C height indicated by the HC agreed well with the frequency of negative (or positive) cloud-to-ground (CG) lightning flashes. This result is consistent with the riming electrification process proposed by Takahashi (1978). As the next step, it is necessary to examine the structure and time series of more complicated systems of thunderclouds to understand the microphysical structure.

In this study, we analyzed a group of thunderclouds in the summer of 2010. We examine the relationship between the polarity of CG flashs and the distribution of hydrometeors not only for the group of thunderclouds but also for each thundercloud.

* Corresponding author address: Takeharu Kouketsu, Hydrospheric Atmospheric Research Center, Nagoya University, Nagoya, 464-8601, Japan; e-mail: Kouketsu@rain.hyarc.nagoya-u.ac.jp.

2. DATA

2.1 X-pol

We use data from an X-pol at Nagoya University, Japan (Fig.1) to observe the group of thunderclouds. The specifications of the X-pol are listed in Table 1. Volume scans were conducted every 6 minutes with 15 elevations from 0.5° to 33.5°.

We obtain four polarimetric variables with the X-pol: radar reflectivity with horizontal polarization (Z_h), differential reflectivity (Z_{dr}), specific differential phase (K_{dp}) and correlation coefficient of horizontally and vertically polarized signals (ρ_{hv}). Each variable is obtained up to 61.8 km from the X-pol with 150 m range resolution and 1.2° beam width. The radar data are interpolated to Cartesian coordinates (Constant Altitude Plan Position Indicator: CAPPI) with 0.5 km horizontal and vertical resolutions using a weighting function (Cressman, 1959). For analysis, we only use radar data up to 60 km from the X-pol to avoid noise around the outer edge of radar range.

2.2 Other data

As supplementary information for HC, we use temperature data from ground observations at Nagoya local meteorological observatory and balloon soundings at Hamamatsu (Fig. 1).

To obtain the polarity and frequency of CG flashes from the thundercloud, we use data from the Lightning Location System (LLS) provided by the Chubu Electric Power Company.

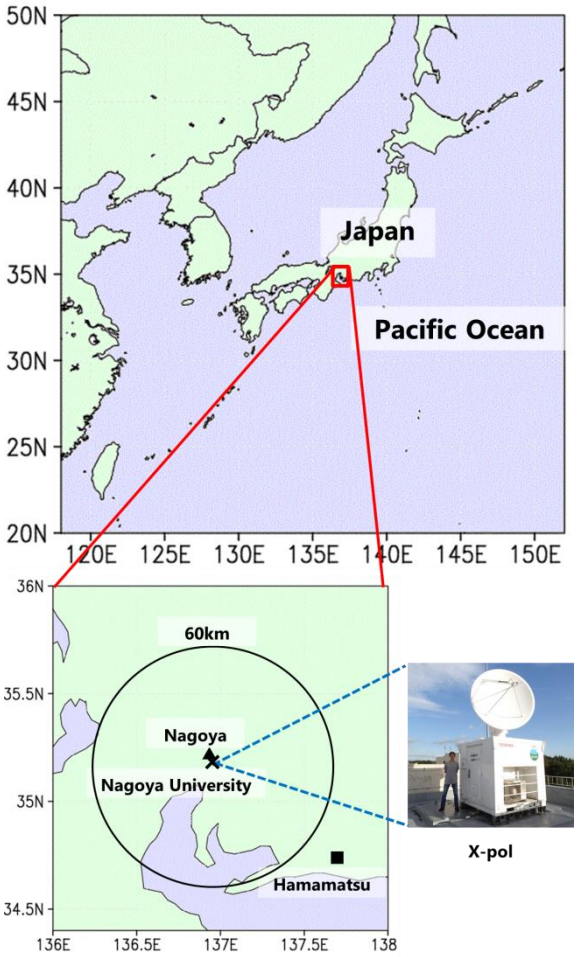

Fig. 1. Locations of Nagoya University X-pol (cross), Nagoya local meteorological observatory (solid triangle) and Hamamatsu, the balloon sounding station (solid square). The black circle shows the range of radar analysis (60 km).

3. HC METHOD

For HC, we use four polarimetric valuables (Z_h, Z_{dr}, K_{dp}, and ρ_{hv}) and temperature as input parameters and obtain the dominant hydrometeor type classified into 10 categories: 1) drizzle, 2) rain, 3) wet snow, 4) dry snow, 5) ice crystal, 6) dry graupel, 7) wet graupel, 8) small hail, 9) large hail and 10) rain and hail.

Our HC method is based on that for S-pol (Liu and Chandrasekar, 2000) with some modifications. We tuned membership functions (MBFs) of K_{dp} in order to adapt to X-pol because the value of K_{dp} depends on wavelength (Bringi and Chandrasekar, 2001). We also tuned the MBF of Z_h for dry graupel, using ground observations in winter.

In addition, we made MBFs for temperature. For some HC categories (drizzle, rain, wet snow, dry snow, ice crystal, and dry graupel), we take account of relative humidity (RH) at the surface because the temperature at which solid hydrometeors melt depends on RH (Matsuo and Sasyo, 1981a, b). In this case, however, it can be assumed that RH = 100% around boundary of solid and liquid hydrometeors because the freezing level (about 5 km) is above cloudbase.

We conducted HC for every grid point of the CAPPI data with 0.5-km horizontal and vertical resolutions, and calculated the volume of the regions where the hydrometeor type was identified as dry snow, ice crystal, dry graupel or wet graupel, by summing volumes of 0.5-km grid points over the entire volume of the target group of thunderclouds.

Table 1. Specifications of the X-pol at Nagoya University.

Frequency		9375 MHz
Antenna size		2.0 m
Beam width		1.2°
Transmitter	Type	Solid state component
	Peak power	200 W
Max range		61.8 km
Pulse width		1 μs (within 5 km) 32 μs (beyond 5 km, pulse compression)
PRF		2000 Hz / 1600 Hz (dual PRF)
Transmission		45° or H only or V only
Rotation rate		3.0 rpm (PPI) , 1.2 rpm (RHI)
Resolution		150 m
Nyquist velocity		16.0 ms^{-1} / 12.8 ms^{-1}

4. CASE OVERVIEW

The group of thunderclouds formed about 40 km

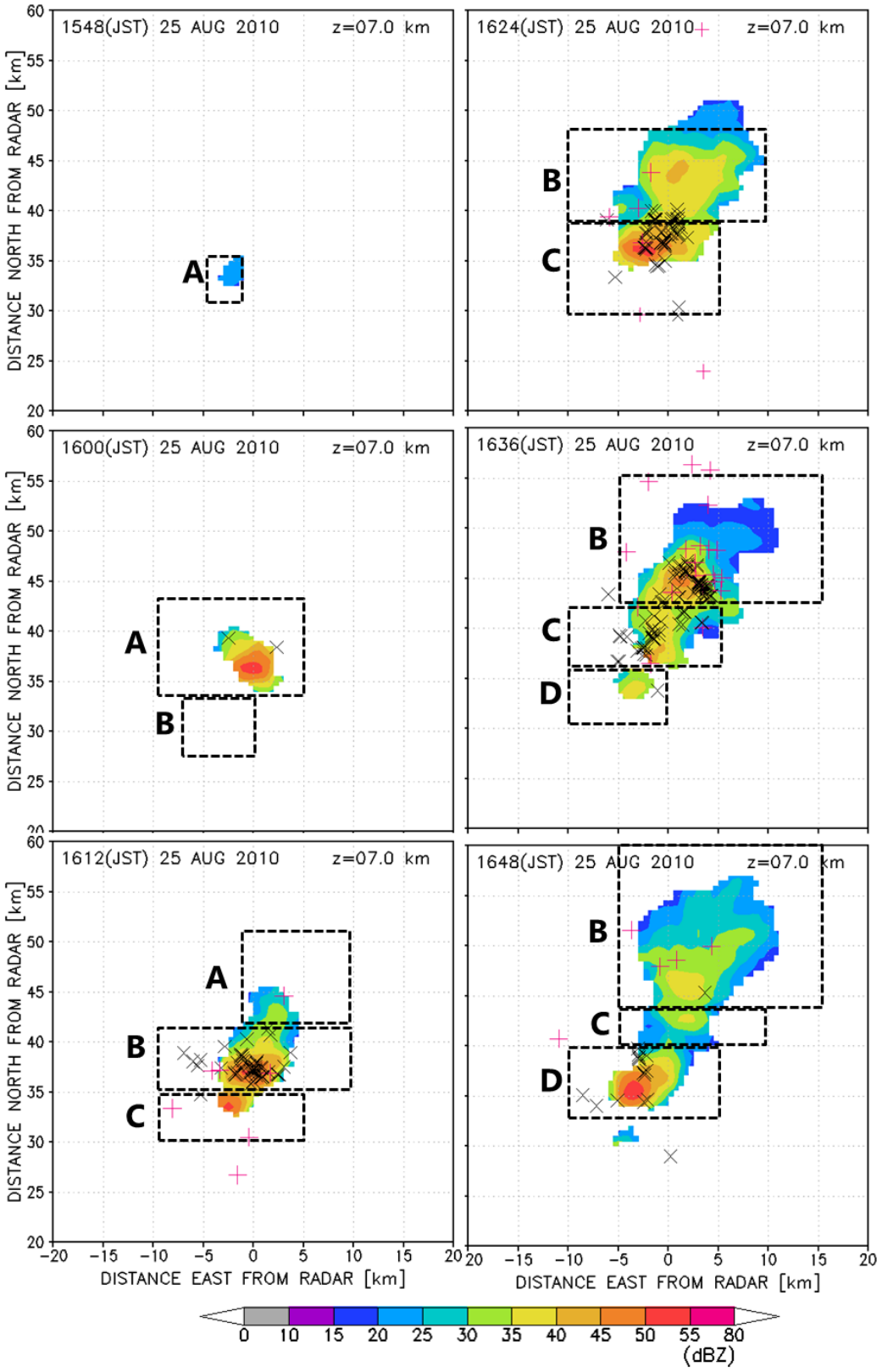

Fig. 2. Time series of Z_h at 7 km height and the locations of positive (pink "+" marks) and negative (black "x" marks) CG flashes from 1600 JST to 1700 JST on August 25, 2010. Rectangles A-D indicate the thundercloud A-D identified in this study.

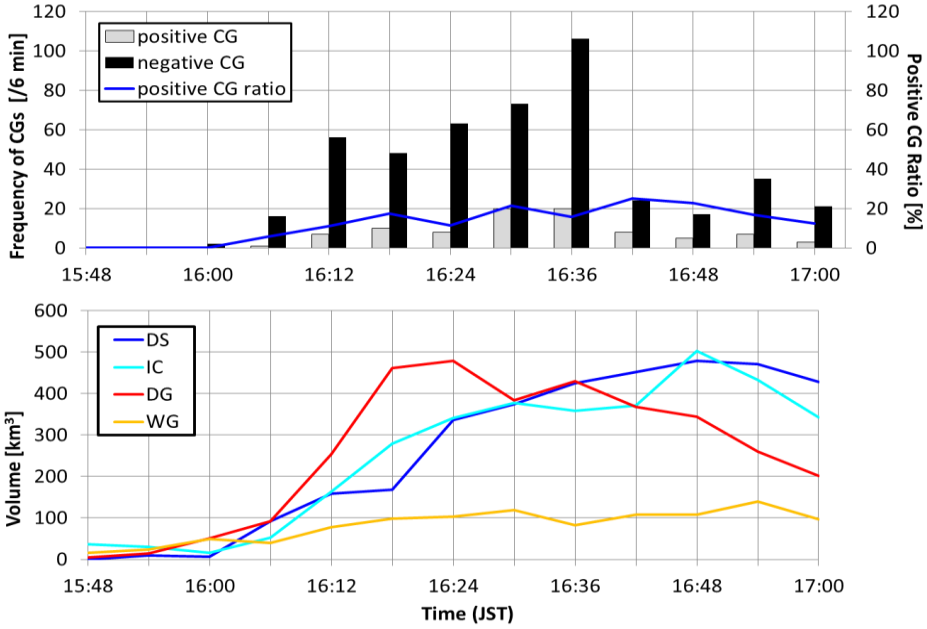

Fig. 3. Time series of the frequency of positive and negative CG flashs, ratio of positive CG flash (upper panel) and volume of region of each hydrometeor type (lower panel) for the target group of thunderclouds. In the lower panel, DS, IC, DG and WG are dry snow, ice crystal, dry graupel, and wet graupel, respectively.

north of the X-pol at Nagoya University around 1548 Japan Standard Time (JST = UTC + 9 hours) on August 25, 2010. It developed deeply and from 1554 JST, echo-top height of 30 dBZ exceeded 7 km. At its peak, it was above 15 km.

Because lightning accompanies deep convection, it is necessary to examine the distribution of solid hydrometeors above 0 °C height. In particular, the existence of graupel around and above -10°C height is critical for negative CG flashes according to riming electrification process (Takahashi, 1978). Therefore, we focus our analysis on the distribution of Z_h at 7 km height (around the -10°C height in this case).

Figure 2 shows time series of Z_h at 7 km height from CAPPI data obtained with the X-pol, and the locations of negative and positive CG flashes. Negative CG flashes were observed mainly below the reflectivity cores, where wet or dry graupel was identified by our HC method. On the other hand, positive CG flashes were observed mainly below the anvil areas, where dry snow or ice crystal was identified because the reflectivity was weak.

From Fig. 2, it can be found that there are four major reflectivity cores, where graupel probably exists. We regard each of them as a “thundercloud” and label them as thundercloud A-D with consideration of spatial distribution and analyze each of them.

First, thundercloud A formed around 1548 JST and moved slowly north-northeastward with the upper air south-southwesterly wind. Then, thundercloud B formed to the southwest of thundercloud A at 1600 JST (at that time, echo-top was below 7 km). Subsequently, thundercloud A decayed and thundercloud C formed to the southwest of thundercloud B. Finally, thundercloud D formed to the southwest of thundercloud C. After 1700 JST, the target group of thunderclouds approached other groups of thunderclouds and we terminated analysis at 1700 JST since the structure was becoming too complex.

5. RESULT

Figure 3 shows time series of frequency of positive and negative CG flashes, and the volume of

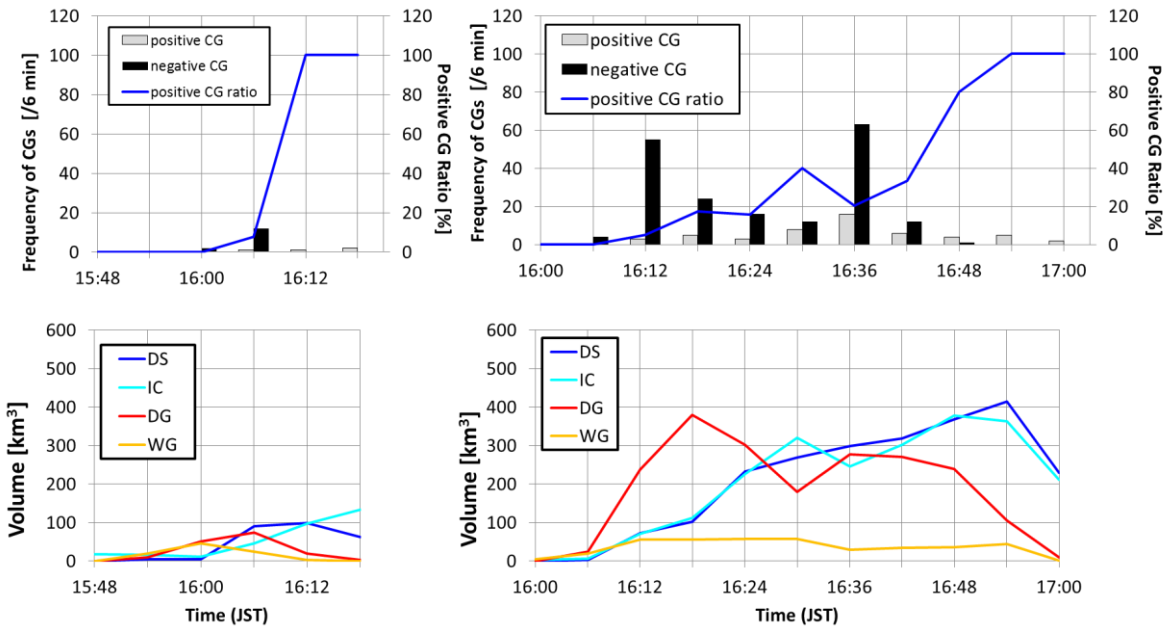

Fig. 4. Same as Fig.3 but for thunderclouds A (left) and B (right).

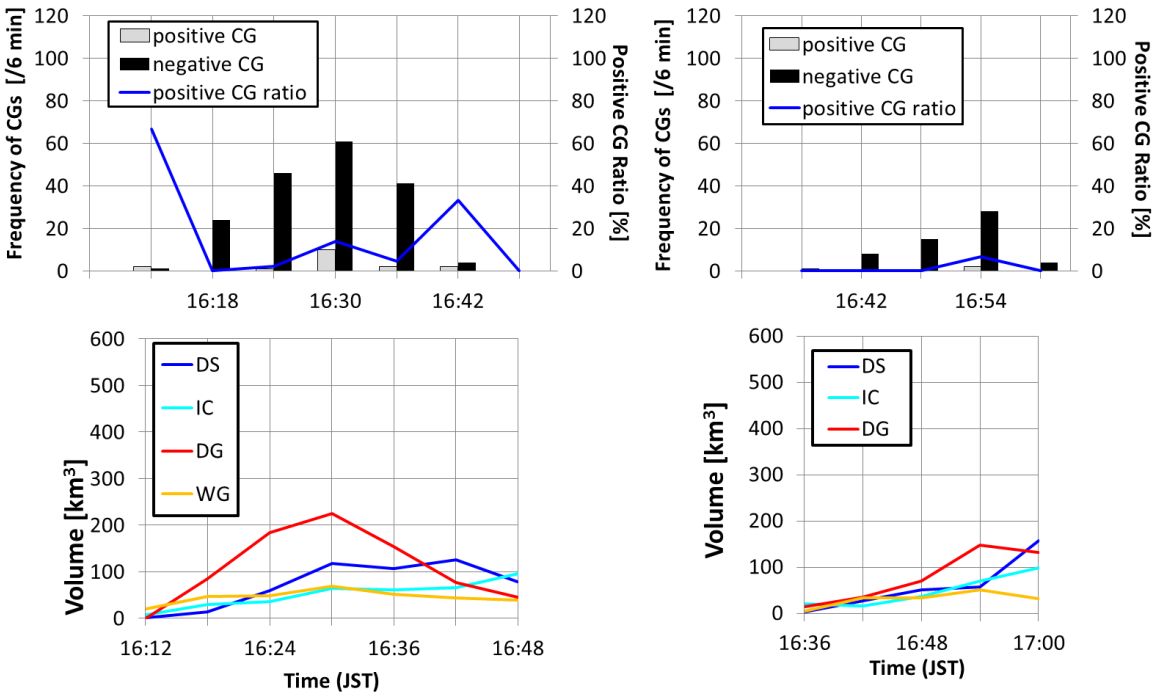

Fig. 5. Same as Fig.3 but for thunderclouds C (left) and D (right).

the region of each hydrometeor type (dry snow, ice crystal, dry graupel, and wet graupel) for the target group of thunderclouds. Negative CG flashes and positive CG flashes were observed from 1600 and 1612 JST, respectively. There were three peaks in frequency of negative CG and positive CG flashes during the analysis period (from 1530 to 1700 JST). The volume of the dry graupel region increased rapidly around the times of the first two peaks in negative CG flash. On the other hand, large volumes

of dry snow and ice crystal regions (≥150 km^3) were identified when positive CG flashes were frequent.

To examine the relationship between the peaks in frequency of positive and negative CG flashes, and the volume of each hydrometeor region, we analyze each of the thunderclouds A-D. For thundercloud A (Fig. 4, left), negative CG flashes were observed from 1600 JST, when the volume of the dry graupel region exceeded 50 km^3. However thundercloud A decayed rapidly and a few positive CG flashes were observed.

For thundercloud B (Fig. 4, right), the first peak in frequency of negative CG flash was observed at 1612 JST, when the volume of dry graupel region was increasing rapidly. After 1618 JST, thundercloud B weakened, but then reintensified and the second peak of frequency of negative CG flash was observed. After that, thundercloud B decayed. Large volumes of dry snow and ice crystal regions (≥200 km^3) were identified, and positive CG flashes were observed.

For thundercloud C (Fig. 5, left), the peak in frequency of negative CG flash was observed when the volume of the dry graupel region reached its maximum.

For thundercloud D (Fig. 5, right), we observed its developing stage and the frequency of negative CG flash increased as the volume of the dry graupel region increased. On the other hand, few positive CG flashes were observed and the volumes of dry snow and ice crystal regions were quite small.

6. DISCUSSION

As mentioned above, negative CG flashes were observed mainly below the reflectivity cores of the group of thunderclouds. In such regions, dry graupel was identified above freezing level (about 5 km in this case). When negative CG flashes were observed, a large amount of dry graupel was identified by HC. On the other hand, positive CG flashes were observed mainly below the anvil areas, which are identified as dry snow or ice crystal by HC because reflectivity was weak. These facts are consistent with the riming electrification process described by Takahashi (1978).

For each of thunderclouds A-D, it also can be found that negative CG flashes were observed when the volume of the dry graupel region identified by HC was quite large (≥50 km^3) and positive CG flashes were observed when each of the volumes of the dry snow and ice crystal regions were large (≥ ~200 km^3). For thundercloud B, the ratio of positive CG flash was much higher than for the other thunderclouds, corresponding to a large amount of dry snow and ice crystal in the anvil.

We have demonstrated that the relationship between the polarity of CG flash and the distribution of hydrometeors (type and amount) was consistent with the riming electrification process described by Takahashi (1978) for not only for the entire of the group of thunderclouds but also for the individual thunderclouds.

7. SUMMARY

We conducted HC for a group of thunderclouds that formed about 40 km north of Nagoya around 1548 JST on 25 August 2010. We examined the microphysical structure of the group of thunderclouds by calculating the volume of regions where dry snow, ice crystal, dry graupel, and wet graupel were identified by our HC method using polarimetric variables (Z_h, Z_{dr}, K_{dp} and ρ_{hv}) and temperature.

A large volume of dry graupel region (≥50 km^3) existed when many negative CG flashes were observed. The volumes of the dry snow and ice crystal regions were large (≥ ~200 km^3) when positive CG flashes were observed. These relationships are consistent with the polarity of CG expected from the riming electrification process. We have shown these relationships hold not only for the group of thunderclouds but also for the individual thunderclouds.

Acknowledgments. The authors are grateful to the Chubu Electric Power Company and Mr. Atsushi Sakakibara (Chuden CTI Co. Ltd.) for providing Lightning Location System (LLS) data. The first author was partly supported by Research Fellow of the Japan Society for the Promotion of Science. This study was also supported by a Grant-in-Aid for Scientific Research of the Japan Society for the

Promotion of Science, and “Formation of a virtual laboratory for diagnosing the earth’s climate system” (VL).

References

Bringi, V. N., and V. Chandrasekar, 2001: Polarimetric Doppler Weather Radar Principals and Applications. Cambridge University Press, 656 pp.

Cressman, G. P., 1959: An operational objective analysis system. Mon. Wea. Rev., 87, 367–374.

Kouketsu, T. and H. Uyeda, 2010: Validation of Hydrometeor Classification Method for X-band Polarimetric Radar Comparison with Ground Observation of Solid Hydrometeor. Proc. Sixth European Conference on Radar in Meteorology and Hydrology (ERAD2010), Advances in Radar Technology, Sibiu, Romania, 195-201.

Kouketsu, T., H. Uyeda, and T. Ohigashi, 2011: Time series of microphysical structure of a thundercloud examined with hydrometeor classification method for X-band polarimetric radar. 35th Conference on Radar Meteorology, Pittsburgh, PA. Manuscript is available: https://ams.confex.com/ams/35Radar/webprogram/Paper191499.html.

Kouketsu, T., M. Oue, T. Ohigashi, K. Tsuboki, H. Minda, H. Uyeda, K. Suzuki, Y. Wakazuki and E. Nakakita, 2013: Validation of Hydrometeor Classification Method for X-band Polarimetric Radars Using Balloon-borne Instruments. Preprints, Conference on MCSs and High-Impact Weather in East Asia (ICMCS-IX), Beijing, China, 337-341.

Liu, H., and V. Chandrasekar, 2000: Classification of Hydrometeors Based on Polarimetric Radar Measurements: Development of Fuzzy Logic and Neuro-Fuzzy Systems, and In Situ Verification. J. Atmos. Oceanic Tech., 17, 140-164.

Matsuo,T., and Y. Sasyo, 1981a: Melting of Snowflakes below Freezing Level in the Atmosphere. J. Met. Soc. Japan, 59, 10-25.

Matsuo,T., and Y. Sasyo, 1981b: Non-Melting Phenomena of Snowflakes Observed in Subsaturated Air below Freezing Level. J. Met. Soc. Japan, 59, 26-32.

Takahashi, T., 1978: Riming Electrification as a Charge Generation Mechanism in Thunderstorms. J. Atmos. Sci., 35, 1536-1548.